Comput Mech (2010) 46:791–803
DOI 10.1007/s00466-010-0518-9

ORIGINAL PAPER

Analysis of plates on Pasternak foundations by radial basis functions

A. J. M. Ferreira · C. M. C. Roque · A. M. A. Neves · R. M. N. Jorge · C. M. M. Soares

Received: 19 February 2010 / Accepted: 22 June 2010 / Published online: 22 July 2010

Abstract This paper addresses the static and free vibration analysis of rectangular plates resting on Pasternak foundations. The Pasternak foundation is described by a two-parameter model. The numerical approach is based on collocation with radial basis functions. The model allows the analysis of arbitrary boundary conditions and irregular geometries. It is shown that the present method, based on a first-order shear deformation theory produces highly accurate displacements and stresses, as well as natural frequencies and modes.

Keywords Plates on Pasternak foundations · Plates on elastic foundations · Plates on Winkler foundations · Free vibrations · Radial basis functions · Collocation

1 Introduction

Many engineering problems can be modeled as isotropic rectangular plates, such as bases of machines, pavement of roads or footing of buildings. One way to describe the behaviour of such plates is the Pasternak (two-parameter) model [1]. The Winkler model [2] can be considered a special case of the Pasternak model.

The analysis of Pasternak plates was conducted previously by several authors, using various approaches. Leissa [3] considered a thin-plate theory, Lam et al. [4] derived the exact solutions of bending, buckling and vibration of a Levy-plate, Xiang et al. [5] derived an analytical vibration solution, Omurtag et al. [6] used the finite element method, Matsunaga [7] developed a special higher-order plate theory, Shen et al. [8] used the the Rayleigh-Ritz method, and Ayvaz et al. [9] used the modified Vlasov model to study the earthquake response of rectangular thin plates on elastic foundation.

In the recent years, some attempts have been made for the vibration analysis of rectangular thick plates on Pasternak foundations. Liew and Teo [10], and Liew et al. [11], Han and Liew [12] used the differential quadrature method to analyse the vibration characteristics of rectangular plates on elastic foundations. Also, Zhou et al. [13] used the Chebyshev polynomials as admissible functions to study the three-dimensional vibration of rectangular plates on elastic foundations by the Ritz method.

Meshless methods are not widely used for the analysis of Mindlin plates on elastic foundations. Civalek [14] used the singular convolution method for the bending analysis of Mindlin plates on elastic foundations. Also, a boundary element method was used by Chucheepsakul and Chinnaboon [15] to analyse plates by a two-parameter model.

Recently, radial basis functions (RBFs) have enjoyed considerable success and research as a technique for interpolating data and functions. A RBFs, $\phi(\|x - x_j\|)$ is a spline that depends on the Euclidian distance from distinct data centers x_j, $j = 1, 2, \ldots, N \in \mathbb{R}^n$, also called nodal or collocation points.

Although most work to date on RBFs relates to scattered data approximation and in general to interpolation theory, there has recently been an increased interest in their use for solving partial differential equations (PDEs). This approach, which approximates the whole solution of the PDE directly

A. J. M. Ferreira (✉) · C. M. C. Roque · A. M. A. Neves · R. M. N. Jorge
Departamento de Engenharia Mecânica, Faculdade de Engenharia da, Universidade do Porto, Rua Dr. Roberto Frias, 4200-465 Porto, Portugal
e-mail: ferreira@fe.up.pt

C. M. M. Soares
Departamento de Engenharia Mecânica, Instituto Superior Técnico, Av. Rovisco Pais, Lisboa, Portugal

using RBFs, is very attractive due to the fact that this is truly a mesh-free technique.

Kansa [16] introduced the concept of solving PDEs using RBFs. Kansa's method is an unsymmetric RBF collocation method based upon the MQ interpolation functions, in which the shape parameter is considered to be variable across the problem domain. The distribution of the shape parameter is obtained by an optimization approach, in which the value of the shape parameter is assumed to be proportional to the curvature of the unknown solution of the original PDE. In this way, it is possible to reduce the condition number of the matrix at the expense of implementing an additional iterative algorithm. In the present work, we implemented the unsymmetric collocation method in its simpler form, without any optimization of the interpolation functions and the collocation points.

The analysis of plates by finite element methods is now fully established. The use of alternative methods such as the meshless methods based on RBFs is atractive due to the absence of a mesh and the ease of collocation methods. The use of RBF for the analysis of structures and materials has been previously studied by numerous authors [17–28]. More recently the authors have applied RBFs to the static deformations of composite beams and plates [29–31].

In this paper it is investigated for the first time the use of RBFs to plates on elastic foundations by the Pasternak model, using a first-order shear deformation theory. The quality of the present method in predicting static deformations, and free vibrations of plates on Winkler and Pasternak foundations is compared and discussed with other methods in some numerical examples.

2 The RBF method

2.1 The static problem

RBF approximations are grid-free numerical schemes that can exploit accurate representations of the boundary, are easy to implement and can be spectrally accurate [32,33].

In this section the formulation of a global unsymmetrical collocation RBF-based method to compute eigenvalues of elliptic operators is presented.

Consider a linear elliptic partial differential operator L and a bounded region Ω in $\mathbb{R}^n$ with some boundary $\partial\Omega$.

The static problems aims the computation of displacements (primary variables) ($\mathbf{u}$) from the global system of equations

$$L\mathbf{u} = \mathbf{f} \text{ in } \Omega \tag{1}$$

$$L_B\mathbf{u} = \mathbf{g} \text{ on } \partial\Omega \tag{2}$$

where L and L_B are linear operators in the domain and on the boundary, respectively. The right-hand side of (1) and (2) represent the external forces applied on the plate and the boundary conditions applied along the perimeter of the plate, respectively. The PDE problem defined in (1) and (2) will be replaced by a finite problem, defined by an algebraic system of equations, after the radial basis expansions.

2.2 The eigenproblem

The eigenproblem looks for eigenvalues (λ) and eigenvectors ($\mathbf{u}$) that satisfy

$$L\mathbf{u} - \lambda\mathbf{u} = 0 \text{ in } \Omega \tag{3}$$

$$L_B\mathbf{u} = 0 \text{ on } \partial\Omega \tag{4}$$

As in the static problem, the eigenproblem defined in (3) and (4) is replaced by a finite-dimensional eigenvalue problem, based on RBF approximations.

2.3 Radial basis functions

The RBF (ϕ) approximation of a function ($\mathbf{u}$) is given by

$$\widetilde{\mathbf{u}}(\mathbf{x}) = \sum_{i=1}^{N} \alpha_i \phi\left(\|x - y_i\|_2\right), \mathbf{x} \in \mathbb{R}^n \tag{5}$$

where $y_i, i = 1, \ldots, N$ is a finite set of distinct points (centers) in $\mathbb{R}^n$. The coefficients α_i are chosen so that $\widetilde{\mathbf{u}}$ satisfies some boundary conditions. The most common RBFs are

$$\begin{aligned}
&\phi(r) = r^3, \quad \text{cubic}\\
&\phi(r) = r^2 \log(r), \quad \text{thin plate splines}\\
&\phi(r) = (1-r)_+^m p(r), \quad \text{Wendland functions}\\
&\phi(r) = e^{-(cr)^2}, \quad \text{Gaussian}\\
&\phi(r) = \sqrt{c^2 + r^2}, \quad \text{multiquadrics}\\
&\phi(r) = (c^2 + r^2)^{-1/2}, \quad \text{inverse multiquadrics}
\end{aligned}$$

where the Euclidian distance r is real and non-negative and c is a shape parameter, a positive constant. In the Wendland functions, $p(r)$ is a polynomial function, which can be defined in various ways. In this paper, the Wendland function was chosen as

$$\phi(r) = (1 - cr)_+^8 \left(32(cr)^3 + 25(cr)^2 + 8cr + 1\right). \tag{6}$$

2.4 Solution of the interpolation problem

Hardy [34] introduced multiquadrics in the analysis of scattered geographical data. In the 1990s Kansa [16] used multiquadrics for the solution of PDEs.

Considering N distinct interpolations, and knowing $u(x_j)$, $j = 1, 2, \ldots, N$, we find α_i by the solution of a $N \times N$ linear system

$$\mathbf{A}\underline{\alpha} = \mathbf{u} \tag{7}$$

where $\mathbf{A} = [\phi(\|x - y_i\|_2)]_{N\times N}$, $\underline{\alpha} = [\alpha_1, \alpha_2, \ldots, \alpha_N]^T$ and $\mathbf{u} = [u(x_1), u(x_2), \ldots, u(x_N)]^T$. The RBF interpolation matrix A is positive definite for some RBFs [35], but in general provides ill-conditioned systems.

2.5 Solution of the static problem

The solution of a static problem by RBFs considers N_I nodes in the domain and N_B nodes on the boundary, with total number of nodes $N = N_I + N_B$.

We denote the sampling points by $x_i \in \Omega, i = 1, \ldots, N_I$ and $x_i \in \partial\Omega, i = N_I + 1, \ldots, N$. At the domain points we solve the following system of equations

$$\sum_{i=1}^{N} \alpha_i L\phi\left(\|x - y_i\|_2\right) = \mathbf{f}(x_j), \quad j = 1, 2, \ldots, N_I \tag{8}$$

or

$$L^I\underline{\alpha} = \mathbf{F} \tag{9}$$

where

$$L^I = \left[L\phi\left(\|x - y_i\|_2\right)\right]_{N_I\times N}. \tag{10}$$

For the boundary conditions we have

$$\sum_{i=1}^{N} \alpha_i L_B\phi\left(\|x - y_i\|_2\right) = \mathbf{g}(x_j), \quad j = N_I + 1, \ldots, N \tag{11}$$

or

$$\mathbf{B}\underline{\alpha} = \mathbf{G}. \tag{12}$$

Therefore we can write a finite-dimensional static problem as

$$\begin{bmatrix} L^I \\ \mathbf{B} \end{bmatrix}\underline{\alpha} = \begin{bmatrix} \mathbf{F}^I \\ \mathbf{G}^I \end{bmatrix} \tag{13}$$

where

$$\mathbf{A}^I = \phi\left[\left(\left\|x_{N_I} - y_j\right\|_2\right)\right]_{N_I\times N},$$
$$\mathbf{B}^I = L_B\phi\left[\left(\|x_{N_I+1} - y_j\|_2\right)\right]_{N_B\times N}.$$

By inverting the system (13), we obtain the vector of $\underline{\alpha}$. We then proceed to the solution by the interpolation equation (5).

2.6 Solution of the eigenproblem

We consider N_I nodes in the interior of the domain and N_B nodes on the boundary, with $N = N_I + N_B$.

We denote interpolation points by $x_i \in \Omega, i = 1, \ldots, N_I$ and $x_i \in \partial\Omega, i = N_I + 1, \ldots, N$. For the interior points we have that

$$\sum_{i=1}^{N} \alpha_i L\phi\left(\|x - y_i\|_2\right) = \lambda\tilde{\mathbf{u}}(x_j), \quad j = 1, 2, \ldots, N_I \tag{14}$$

or

$$L^I\underline{\alpha} = \lambda\tilde{\mathbf{u}}^I \tag{15}$$

where

$$L^I = \left[L\phi\left(\|x - y_i\|_2\right)\right]_{N_I\times N} \tag{16}$$

For the boundary conditions we have

$$\sum_{i=1}^{N} \alpha_i L_B\phi\left(\|x - y_i\|_2\right) = 0, \quad j = N_I + 1, \ldots, N \tag{17}$$

or

$$\mathbf{B}\underline{\alpha} = 0. \tag{18}$$

Therefore we can write a finite-dimensional problem as a generalized eigenvalue problem

$$\begin{bmatrix} L^I \\ \mathbf{B} \end{bmatrix}\underline{\alpha} = \lambda\begin{bmatrix} \mathbf{A}^I \\ \mathbf{0} \end{bmatrix}\underline{\alpha} \tag{19}$$

where

$$\mathbf{A}^I = \phi\left[\left(\left\|x_{N_I} - y_j\right\|_2\right)\right]_{N_I\times N},$$
$$\mathbf{B}^I = L_B\phi\left[\left(\left\|x_{N_I+1} - y_j\right\|_2\right)\right]_{N_B\times N}$$

We seek the generalized eigenvalues and eigenvectors of these matrices.

In this paper we follow a second algorithm (see [36] for details) that can be formulated as follows. We can write

$$\underline{\alpha} = \underline{\mathbf{A}}^{-1}\begin{bmatrix} \underline{\mathbf{u}}^I \\ \mathbf{0}_{N_B\times 1} \end{bmatrix} \tag{20}$$

where $\mathbf{0}_{p\times q}$ is a $p \times q$ zero matrix, and

$$\underline{\mathbf{A}} = \begin{bmatrix} \mathbf{A}^I \\ \mathbf{B} \end{bmatrix} \tag{21}$$

We can write a standard eigenvalue problem as

$$L_\phi\underline{\mathbf{u}}^I = \lambda\underline{\mathbf{u}}^I \tag{22}$$

where L_ϕ is a $N_I \times N_I$ matrix given by

$$L_\phi = L^I\underline{\mathbf{A}}^{-1}\begin{bmatrix} I_{N_I\times N_I} \\ \mathbf{0}_{N_B\times N_I} \end{bmatrix} \tag{23}$$

The RBF approximation of the eigenpairs of (3)–(4) is now obtained by computing the eigenvalues and eigenvectors of the matrix L_ϕ. The eigenproblem (22) has dimension $N_I \times N_I$ whereas eigenproblem (19) has dimension $N \times N$. However in (22) we need to invert matrix $\underline{\mathbf{A}}$, which represents an extra computing cost when compared to (19).

3 Static and free vibration analysis of plates on Pasternak foundations

3.1 Equations of motion and boundary conditions

Based on the FSDT (first-order shear deformation theory), the transverse displacement $w(x, y, t)$ and the rotations $\theta_x(x, y, t)$ and $\theta_y(x, y, t)$ about the $y-$ and $x-$axes as functions of time, t, are independently interpolated due to uncoupling between inplane displacements and bending displacements for plates on Pasternak foundations. The equations of motion for the free vibration of plates on Pasternak foundations [10–12] are:

$$D_{11}\frac{\partial^2\theta_x}{\partial x^2} + D_{16}\frac{\partial^2\theta_y}{\partial x^2} + (D_{12}+D_{66})\frac{\partial^2\theta_y}{\partial x\partial y} + 2D_{16}\frac{\partial^2\theta_x}{\partial x\partial y} + D_{66}\frac{\partial^2\theta_x}{\partial y^2} + D_{26}\frac{\partial^2\theta_y}{\partial y^2} - kA_{45}\left(\theta_y + \frac{\partial w}{\partial y}\right) - kA_{55}\left(\theta_x + \frac{\partial w}{\partial x}\right) = I_2\frac{\partial^2\theta_x}{\partial t^2} \tag{24}$$

$$D_{16}\frac{\partial^2\theta_x}{\partial x^2} + D_{66}\frac{\partial^2\theta_y}{\partial x^2} + (D_{12}+D_{66})\frac{\partial^2\theta_x}{\partial x\partial y} + 2D_{26}\frac{\partial^2\theta_y}{\partial x\partial y} + D_{26}\frac{\partial^2\theta_x}{\partial y^2} + D_{22}\frac{\partial^2\theta_y}{\partial y^2} - kA_{44}\left(\theta_y + \frac{\partial w}{\partial y}\right) - kA_{45}\left(\theta_x + \frac{\partial w}{\partial x}\right) = I_2\frac{\partial^2\theta_y}{\partial t^2} \tag{25}$$

$$\frac{\partial}{\partial x}\left[kA_{45}\left(\theta_y + \frac{\partial w}{\partial y}\right) + kA_{55}\left(\theta_x + \frac{\partial w}{\partial x}\right)\right] + \frac{\partial}{\partial y}\left[kA_{44}\left(\theta_y + \frac{\partial w}{\partial y}\right) + kA_{45}\left(\theta_x + \frac{\partial w}{\partial x}\right)\right] - k_f w + G_f\left(\frac{\partial^2 w}{\partial x^2} + \frac{\partial^2 w}{\partial y^2}\right) + q = I_0\frac{\partial^2 w}{\partial t^2} \tag{26}$$

where q is the external applied load, D_{ij} and A_{ij} are the bending and shear stiffness components, and I_i are the mass inertias defined as [37]

$$I_0 = \int_{-\frac{h}{2}}^{\frac{h}{2}} \rho dz, \quad I_2 = \int_{-\frac{h}{2}}^{\frac{h}{2}} \rho z^2 dz. \tag{27}$$

Here ρ and h denote the density and the total thickness of the plate, respectively. Also, k_f is the Winkler foundation stiffness while G_f is the shear stiffness of the elastic foundation. The Winkler foundation can be considered as a special case of the Pasternak foundation where a shear interaction between the spring elements is assumed. The shear correction factor, k, is here taken as $5/6$, by assuming a rectangular cross-section of the plate.

The bending moments and shear forces are expressed as functions of the displacement gradients and the material constitutive equations by

$$M_x = D_{11}\frac{\partial\theta_x}{\partial x} + D_{12}\frac{\partial\theta_y}{\partial y} + D_{16}\left(\frac{\partial\theta_x}{\partial y} + \frac{\partial\theta_y}{\partial x}\right) \tag{28}$$

$$M_y = D_{12}\frac{\partial\theta_x}{\partial x} + D_{22}\frac{\partial\theta_y}{\partial y} + D_{26}\left(\frac{\partial\theta_x}{\partial y} + \frac{\partial\theta_y}{\partial x}\right) \tag{29}$$

$$M_{xy} = D_{16}\frac{\partial\theta_x}{\partial x} + D_{26}\frac{\partial\theta_y}{\partial y} + D_{66}\left(\frac{\partial\theta_x}{\partial y} + \frac{\partial\theta_y}{\partial x}\right) \tag{30}$$

$$Q_x = kA_{55}\left(\theta_x + \frac{\partial w}{\partial x}\right) + kA_{45}\left(\theta_y + \frac{\partial w}{\partial y}\right) \tag{31}$$

$$Q_y = kA_{45}\left(\theta_x + \frac{\partial w}{\partial x}\right) + kA_{55}\left(\theta_y + \frac{\partial w}{\partial y}\right) \tag{32}$$

For free vibration problems we set $q = 0$, and assume harmonic solution in terms of displacements w, θ_x, θ_y in the form

$$w(x, y, t) = W(w, y)e^{i\omega t} \tag{33}$$

$$\theta_x(x, y, t) = \Psi_x(w, y)e^{i\omega t} \tag{34}$$

$$\theta_y(x, y, t) = \Psi_y(w, y)e^{i\omega t} \tag{35}$$

where ω is the frequency of natural vibration. Substituting the harmonic expansion into equations of motion we obtain the following equations in terms of the amplitudes W, Ψ_x, Ψ_y

$$D_{11}\frac{\partial^2\Psi_x}{\partial x^2} + D_{16}\frac{\partial^2\Psi_y}{\partial x^2} + (D_{12}+D_{66})\frac{\partial^2\Psi_y}{\partial x\partial y} + 2D_{16}\frac{\partial^2\Psi_x}{\partial x\partial y} + D_{66}\frac{\partial^2\Psi_x}{\partial y^2} + D_{26}\frac{\partial^2\Psi_y}{\partial y^2} - kA_{45}\left(\Psi_y + \frac{\partial W}{\partial y}\right) - kA_{55}\left(\Psi_x + \frac{\partial W}{\partial x}\right) = -I_2\omega^2\Psi_x \tag{36}$$

$$D_{16}\frac{\partial^2\Psi_x}{\partial x^2} + D_{66}\frac{\partial^2\Psi_y}{\partial x^2} + (D_{12}+D_{66})\frac{\partial^2\Psi_x}{\partial x\partial y} + 2D_{26}\frac{\partial^2\Psi_y}{\partial x\partial y} + D_{26}\frac{\partial^2\Psi_x}{\partial y^2} + D_{22}\frac{\partial^2\Psi_y}{\partial y^2} - kA_{44}\left(\Psi_y + \frac{\partial W}{\partial y}\right) - kA_{45}\left(\Psi_x + \frac{\partial W}{\partial x}\right) = -I_2\omega^2\Psi_y \tag{37}$$

$$\frac{\partial}{\partial x}\left[kA_{45}\left(\Psi_y + \frac{\partial W}{\partial y}\right) + kA_{55}\left(\Psi_x + \frac{\partial W}{\partial x}\right)\right] + \frac{\partial}{\partial y}\left[kA_{44}\left(\Psi_y + \frac{\partial W}{\partial y}\right) + kA_{45}\left(\Psi_x + \frac{\partial W}{\partial x}\right)\right] - k_f W + G_f\left(\frac{\partial^2 W}{\partial x^2} + \frac{\partial^2 W}{\partial y^2}\right) = -I_0\omega^2 W. \tag{38}$$

The boundary conditions for an arbitrary edge with simply supported, clamped and free edge conditions are as follows:

(a) Simply supported

- SS1, $w = 0;\ M_n = 0;\ M_{ns} = 0$
- SS2, $w = 0;\ M_n = 0;\ \theta_s = 0$

(b) Clamped, $w = 0;\ \theta_n = 0;\ \theta_s = 0$

(c) Free, $Q_n = 0;\ M_n = 0;\ M_{ns} = 0$

In previous equations, the subscripts n and s refer to the normal and tangential directions of the edge, respectively; M_n, M_{ns} and Q_n represent the normal bending moment, twisting moment and shear force on the plate edge; θ_n and θ_s represent the rotations about the tangential and normal coordinates at the plate edge.

The stress resultants on an edge whose normal is represented by $\mathbf{n} = (n_x, n_y)$ can be expressed as

$$M_n = n_x^2 M_x + 2n_x n_y M_{xy} + n_y^2 M_y \tag{39}$$

$$M_{ns} = \left(n_x^2 - n_y^2\right) M_{xy} - n_x n_y (My - Mx) \tag{40}$$

$$Q_n = n_x Q_x + n_y Q_y \tag{41}$$

$$\theta_n = n_x \theta_x + n_y \theta_y \tag{42}$$

$$\theta_s = n_x \theta_y - n_y \theta_x \tag{43}$$

where n_x and n_y are the direction cosines of a unit normal vector at a point at the laminated plate boundary [37,38].

4 Discretization of the equations of motion and boundary conditions

The radial basis collocation method follows a simple implementation procedure. Taking Eq. (13), we compute

$$\alpha = \begin{bmatrix} L^I \\ \mathbf{B} \end{bmatrix}^{-1} \begin{bmatrix} \mathbf{F}^I \\ \mathbf{G}^I \end{bmatrix} \tag{44}$$

This α vector is then used to obtain solution $\tilde{\mathbf{u}}$, by using (7). If derivatives of $\tilde{\mathbf{u}}$ are needed, such derivatives are computed as

$$\frac{\partial \tilde{\mathbf{u}}}{\partial x} = \sum_{j=1}^{N} \alpha_j \frac{\partial \phi_j}{\partial x} \tag{45}$$

$$\frac{\partial^2 \tilde{\mathbf{u}}}{\partial x^2} = \sum_{j=1}^{N} \alpha_j \frac{\partial^2 \phi_j}{\partial x^2}, \text{ etc.} \tag{46}$$

The equations of motion and the boundary conditions can now be discretized according to the RBF collocation, as

$$\begin{aligned}
&D_{11} \sum_{j=1}^{N} \alpha_j^{\Psi_x} \frac{\partial^2 \phi_j}{\partial x^2} + D_{16} \sum_{j=1}^{N} \alpha_j^{\Psi_y} \frac{\partial^2 \phi_j}{\partial x^2} \\
&\quad + (D_{12} + D_{66}) \sum_{j=1}^{N} \alpha_j^{\Psi_y} \frac{\partial^2 \phi_j}{\partial x \partial y} \\
&\quad + 2D_{16} \sum_{j=1}^{N} \alpha_j^{\Psi_x} \frac{\partial^2 \phi_j}{\partial x \partial y} + D_{66} \sum_{j=1}^{N} \alpha_j^{\Psi_x} \frac{\partial^2 \phi_j}{\partial y^2} \\
&\quad + D_{26} \sum_{j=1}^{N} \alpha_j^{\Psi_y} \frac{\partial^2 \phi_j}{\partial y^2} \\
&\quad - kA_{45} \left(\sum_{j=1}^{N} \alpha_j^{\Psi_y} \phi_j + \sum_{j=1}^{N} \alpha_j^{W} \frac{\partial \phi_j}{\partial y} \right) \\
&\quad - kA_{55} \left(\sum_{j=1}^{N} \alpha_j^{\Psi_x} \phi_j + \sum_{j=1}^{N} \alpha_j^{W} \frac{\partial \phi_j}{\partial x} \right) \\
&= -I_2 \omega^2 \sum_{j=1}^{N} \alpha_j^{\Psi_x} \phi_j
\end{aligned} \tag{47}$$

$$\begin{aligned}
&D_{16} \sum_{j=1}^{N} \alpha_j^{\Psi_x} \frac{\partial^2 \phi_j}{\partial x^2} + D_{66} \sum_{j=1}^{N} \alpha_j^{\Psi_y} \frac{\partial^2 \phi_j}{\partial x^2} \\
&\quad + (D_{12} + D_{66}) \sum_{j=1}^{N} \alpha_j^{\Psi_x} \frac{\partial^2 \phi_j}{\partial x \partial y} \\
&\quad + 2D_{26} \sum_{j=1}^{N} \alpha_j^{\Psi_y} \frac{\partial^2 \phi_j}{\partial x \partial y} + D_{26} \sum_{j=1}^{N} \alpha_j^{\Psi_x} \frac{\partial^2 \phi_j}{\partial y^2} \\
&\quad + D_{22} \sum_{j=1}^{N} \alpha_j^{\Psi_y} \frac{\partial^2 \phi_j}{\partial y^2} \\
&\quad - kA_{44} \left(\sum_{j=1}^{N} \alpha_j^{\Psi_y} \phi_j + \sum_{j=1}^{N} \alpha_j^{W} \frac{\partial \phi_j}{\partial y} \right) \\
&\quad - kA_{45} \left(\sum_{j=1}^{N} \alpha_j^{\Psi_x} \phi_j + \sum_{j=1}^{N} \alpha_j^{W} \frac{\partial \phi_j}{\partial x} \right) \\
&= -I_2 \omega^2 \sum_{j=1}^{N} \alpha_j^{\Psi_y} \phi_j
\end{aligned} \tag{48}$$

$$\begin{aligned}
&\frac{\partial}{\partial x} \left[kA_{45} \left(\sum_{j=1}^{N} \alpha_j^{\Psi_y} \phi_j + \sum_{j=1}^{N} \alpha_j^{W} \frac{\partial \phi_j}{\partial y} \right) \right. \\
&\quad \left. + kA_{55} \left(\sum_{j=1}^{N} \alpha_j^{\Psi_x} \phi_j + \sum_{j=1}^{N} \alpha_j^{W} \frac{\partial \phi_j}{\partial x} \right) \right] \\
&\quad + \frac{\partial}{\partial y} \left[kA_{44} \left(\sum_{j=1}^{N} \alpha_j^{\Psi_y} \phi_j + \sum_{j=1}^{N} \alpha_j^{W} \frac{\partial \phi_j}{\partial y} \right) \right.
\end{aligned}$$

Table 1 Convergence study for deflections, moments and shear forces of uniformly loaded square CCCC plates on Winkler foundations ($K = 1$; $\nu = 0.3$)

h/a	Grid (points)	w ($\times 10^{-3} qa^4/D$) $x = y = 0$	M_{xx} ($\times 10^{-2} qa^2/D$) $x = y = 0$	M_{yy} ($\times 10^{-2} qa^2/D$) $x = y = 0$	M_{xy} ($\times 10^{-2} qa^2/D$) $x = y = -1$	Q_x ($\times qa$) $x = 0$; $y = -1$	Q_y ($\times qa$) $x = -1$, $y = 0$
0.01	13 × 13	1.783	2.390	3.300	0.062	0.133	−0.648
	17 × 17	1.924	2.441	3.292	0.190	0.206	−0.507
	21 × 21	1.819	1.978	2.592	0.156	0.832	−0.225
	25 × 25	1.965	2.500	3.548	0.101	0.284	−0.512
	29 × 29	1.918	2.414	3.333	0.102	0.233	−0.513
	33 × 33	1.918	2.437	3.319	0.101	0.246	−0.515
0.05	13 × 13	1.990	2.454	3.276	0.463	0.239	−0.515
	17 × 17	1.989	2.471	3.319	0.465	0.244	−0.509
	21 × 21	1.989	2.473	3.321	0.468	0.245	−0.509
	25 × 25	1.989	2.472	3.322	0.466	0.245	−0.509
0.1	13 × 13	2.204	2.561	3.282	0.849	0.246	−0.502
	17 × 17	2.205	2.573	3.317	0.849	0.248	−0.500
	21 × 21	2.206	2.575	3.321	0.851	0.248	−0.500
	25 × 25	2.206	2.575	3.321	0.850	0.248	−0.500
0.2	13 × 13	3.014	2.910	3.283	1.432	0.256	−0.476
	17 × 17	3.015	2.914	3.296	1.432	0.256	−0.475
	21 × 21	3.015	2.914	3.298	1.433	0.256	−0.474
	25 × 25	3.015	2.915	3.298	1.433	0.256	−0.474

Table 2 Convergence study for deflections, moments and shear forces of uniformly loaded square CCCC plates on Winkler foundations ($K = 3$; $\nu = 0.3$)

h/a	Grid (points)	w ($\times 10^{-3} qa^4/D$) $x = y = 0$	M_{xx} ($\times 10^{-2} qa^2/D$) $x = y = 0$	M_{yy} ($\times 10^{-2} qa^2/D$) $x = y = 0$	M_{xy} ($\times 10^{-2} qa^2/D$) $x = y = -1$	Q_x ($\times qa$) $x = 0$; $y = -1$	Q_y ($\times qa$) $x = -1$, $y = 0$
0.01	13 × 13	1.629	2.161	2.991	0.059	0.125	−0.607
	17 × 17	1.750	2.187	2.962	0.179	0.194	−0.474
	21 × 21	1.656	1.759	2.313	0.148	0.785	−0.208
	25 × 25	1.785	2.239	3.197	0.095	0.267	−0.477
	29 × 29	1.745	2.163	3.001	0.097	0.219	−0.479
	33 × 33	1.744	2.184	2.988	0.095	0.231	−0.481
0.05	13 × 13	1.803	2.189	2.936	0.434	0.224	−0.480
	17 × 17	1.803	2.206	2.976	0.436	0.229	−0.474
	21 × 21	1.802	2.208	2.978	0.439	0.229	−0.474
	25 × 25	1.803	2.207	2.979	0.437	0.230	−0.474
0.1	13 × 13	1.975	2.258	2.905	0.786	0.229	−0.464
	17 × 17	1.976	2.270	2.937	0.787	0.230	−0.462
	21 × 21	1.976	2.272	2.941	0.788	0.231	−0.462
	25 × 25	1.976	2.272	2.941	0.787	0.231	−0.462
0.2	13 × 13	2.589	2.459	2.777	1.276	0.232	−0.426
	17 × 17	2.590	2.462	2.789	1.277	0.232	−0.425
	21 × 21	2.590	2.463	2.790	1.278	0.231	−0.425
	25 × 25	2.590	2.463	2.790	1.278	0.232	−0.425

Table 3 Convergence study for deflections, moments and shear forces of uniformly loaded square CCCC plates on Winkler foundations ($K = 5$; $\nu = 0.3$)

h/a	Grid (points)	w ($\times 10^{-3} qa^4/D$) $x = y = 0$	M_{xx} ($\times 10^{-2} qa^2/D$) $x = y = 0$	M_{yy} ($\times 10^{-2} qa^2/D$) $x = y = 0$	M_{xy} ($\times 10^{-2} qa^2/D$) $x = y = -1$	Q_x ($\times qa$) $x = 0$; $y = -1$	Q_y ($\times qa$) $x = -1$, $y = 0$
0.01	13 × 13	1.016	1.258	1.772	0.045	0.091	−0.443
	17 × 17	1.071	1.211	1.688	0.137	0.144	−0.343
	21 × 21	1.018	0.910	1.227	0.114	0.600	−0.140
	25 × 25	1.090	1.238	1.848	0.073	0.199	−0.342
	29 × 29	1.069	1.195	1.718	0.074	0.164	−0.346
	33 × 33	1.069	1.212	1.709	0.073	0.173	−0.347
0.05	13 × 13	1.088	1.188	1.643	0.324	0.167	−0.343
	17 × 17	1.088	1.203	1.672	0.325	0.170	−0.340
	21 × 21	1.088	1.205	1.673	0.327	0.170	−0.339
	25 × 25	1.088	1.204	1.674	0.326	0.171	−0.340
0.1	13 × 13	1.140	1.170	1.545	0.555	0.166	−0.324
	17 × 17	1.141	1.180	1.567	0.556	0.167	−0.322
	21 × 21	1.141	1.181	1.569	0.557	0.167	−0.322
	25 × 25	1.141	1.181	1.569	0.556	0.167	−0.322
0.2	13 × 13	1.289	1.095	1.245	0.787	0.155	−0.271
	17 × 17	1.289	1.097	1.251	0.788	0.155	−0.270
	21 × 21	1.289	1.098	1.252	0.789	0.154	−0.269
	25 × 25	1.289	1.098	1.252	0.788	0.154	−0.269

Table 4 Convergence study for deflections, moments and shear forces of uniformly loaded square SSSS plates on Winkler foundations ($K = 1$; $\nu = 0.3$)

h/a	Grid (points)	w ($\times 10^{-3} qa^4/D$) $x = y = 0$	M_{xx} ($\times 10^{-2} qa^2/D$) $x = y = 0$	M_{yy} ($\times 10^{-2} qa^2/D$) $x = y = 0$	M_{xy} ($\times 10^{-2} qa^2/D$) $x = y = -1$	Q_x ($\times qa$) $x = 0$; $y = -1$	Q_y ($\times qa$) $x = -1$, $y = 0$
0.01	13 × 13	3.957	4.664	4.664	2.832	0.378	−0.378
	17 × 17	4.046	4.753	4.754	3.224	0.336	−0.335
	21 × 21	4.063	4.780	4.780	3.242	0.337	−0.335
	25 × 25	4.049	4.770	4.770	3.237	0.333	−0.331
	29 × 29	4.054	4.775	4.775	3.240	0.336	−0.336
	33 × 33	4.054	4.775	4.775	3.241	0.337	−0.337
0.05	13 × 13	4.100	4.751	4.751	3.237	0.338	−0.338
	17 × 17	4.103	4.773	4.773	3.241	0.337	−0.337
	21 × 21	4.104	4.775	4.775	3.240	0.337	−0.337
	25 × 25	4.104	4.775	4.775	3.241	0.337	−0.337
0.1	13 × 13	4.258	4.760	4.760	3.241	0.338	−0.338
	17 × 17	4.261	4.773	4.773	3.241	0.337	−0.337
	21 × 21	4.261	4.774	4.774	3.240	0.337	−0.337
	25 × 25	4.261	4.774	4.774	3.240	0.337	−0.337
0.2	13 × 13	4.887	4.768	4.768	3.241	0.338	−0.338
	17 × 17	4.888	4.771	4.771	3.240	0.337	−0.337
	21 × 21	4.888	4.772	4.772	3.238	0.337	−0.337
	25 × 25	4.888	4.772	4.772	3.239	0.337	−0.337

Table 5 Convergence study for deflections, moments and shear forces of uniformly loaded square SSSS plates on Winkler foundations ($K = 3$; $\nu = 0.3$)

h/a	Grid (points)	w ($\times 10^{-3} qa^4/D$) $x = y = 0$	M_{xx} ($\times 10^{-2} qa^2/D$) $x = y = 0$	M_{yy} ($\times 10^{-2} qa^2/D$) $x = y = 0$	M_{xy} ($\times 10^{-2} qa^2/D$) $x = y = -1$	Q_x ($\times qa$) $x = 0$; $y = -1$	Q_y ($\times qa$) $x = -1$, $y = 0$
0.01	13 × 13	3.270	3.785	3.785	2.354	0.335	−0.335
	17 × 17	3.343	3.855	3.856	2.736	0.292	−0.291
	21 × 21	3.356	3.878	3.878	2.751	0.293	−0.291
	25 × 25	3.345	3.871	3.872	2.748	0.289	−0.287
	29 × 29	3.349	3.875	3.875	2.751	0.292	−0.292
	33 × 33	3.349	3.875	3.875	2.751	0.293	−0.293
0.05	13 × 13	3.378	3.843	3.843	2.743	0.294	−0.294
	17 × 17	3.381	3.863	3.863	2.746	0.292	−0.292
	21 × 21	3.381	3.865	3.865	2.745	0.292	−0.292
	25 × 25	3.381	3.865	3.865	2.745	0.292	−0.292
0.1	13 × 13	3.481	3.821	3.821	2.729	0.292	−0.292
	17 × 17	3.483	3.833	3.833	2.729	0.291	−0.291
	21 × 21	3.483	3.834	3.834	2.727	0.291	−0.291
	25 × 25	3.483	3.834	3.834	2.728	0.291	−0.291
0.2	13 × 13	3.871	3.713	3.713	2.662	0.286	−0.286
	17 × 17	3.873	3.715	3.715	2.661	0.285	−0.285
	21 × 21	3.873	3.716	3.716	2.659	0.285	−0.285
	25 × 25	3.873	3.716	3.716	2.660	0.285	−0.285

Table 6 Convergence study for deflections, moments and shear forces of uniformly loaded square SSSS plates on Winkler foundations ($K = 5$; $\nu = 0.3$)

h/a	Grid (points)	w ($\times 10^{-3} qa^4/D$) $x = y = 0$	M_{xx} ($\times 10^{-2} qa^2/D$) $x = y = 0$	M_{yy} ($\times 10^{-2} qa^2/D$) $x = y = 0$	M_{xy} ($\times 10^{-2} qa^2/D$) $x = y = -1$	Q_x ($\times qa$) $x = 0$; $y = -1$	Q_y ($\times qa$) $x = -1$, $y = 0$
0.01	13 × 13	1.471	1.502	1.502	1.098	0.221	−0.221
	17 × 17	1.503	1.525	1.526	1.450	0.175	−0.175
	21 × 21	1.509	1.539	1.539	1.460	0.177	−0.174
	25 × 25	1.504	1.539	1.540	1.461	0.173	−0.171
	29 × 29	1.506	1.540	1.540	1.461	0.176	−0.176
	33 × 33	1.506	1.540	1.540	1.462	0.176	−0.176
0.05	13 × 13	1.508	1.507	1.507	1.451	0.177	−0.177
	17 × 17	1.509	1.524	1.524	1.453	0.176	−0.176
	21 × 21	1.509	1.525	1.525	1.451	0.176	−0.176
	25 × 25	1.509	1.526	1.526	1.452	0.176	−0.176
0.1	13 × 13	1.518	1.471	1.471	1.423	0.174	−0.174
	17 × 17	1.519	1.480	1.480	1.422	0.173	−0.173
	21 × 21	1.519	1.482	1.482	1.420	0.173	−0.173
	25 × 25	1.519	1.482	1.482	1.421	0.173	−0.173
0.2	13 × 13	1.550	1.326	1.326	1.313	0.163	−0.163
	17 × 17	1.551	1.327	1.327	1.312	0.162	−0.162
	21 × 21	1.551	1.328	1.328	1.310	0.162	−0.162
	25 × 25	1.551	1.328	1.328	1.311	0.162	−0.162

Table 7 Deflections, moments and shear forces of uniformly loaded square SS plates on Winkler foundations ($\nu = 0.3$)

K	h/a	Method	w $(\times 10^{-3}qa^4/D)$ $x = y = 0$	M_{xx} $(\times 10^{-2}qa^2/D)$ $x = y = 0$	M_{yy} $(\times 10^{-2}qa^2/D)$ $x = y = 0$	M_{xy} $(\times 10^{-2}qa^2/D)$ $x = y = -1$	Q_x $(\times qa)$ $x = 0; y = -1$	Q_y (xqa) $x = -1, y = 0$
1	0.01	Present (21 × 21 points)	4.050	4.776	4.784	3.234	0.334	−0.341
		Kobayashi and Sonoda [39]	4.054	4.775	4.775	3.241	0.337	−0.337
	0.05	Present (21 × 21 points)	4.104	4.775	4.775	3.241	0.337	−0.337
		Kobayashi and Sonoda [39]	4.104	4.775	4.775	3.241	0.337	−0.337
	0.1	Present (21 × 21 points)	4.261	4.774	4.774	3.240	0.337	−0.337
		Kobayashi and Sonoda [39]	4.261	4.774	4.774	3.240	0.337	−0.337
	0.2	Present (21 × 21 points)	4.888	4.772	4.772	3.239	0.337	−0.337
		Kobayashi and Sonoda [39]	4.888	4.772	4.772	3.239	0.337	−0.337
3	0.01	Present (21 × 21 points)	3.345	3.877	3.885	2.745	0.290	−0.297
		Kobayashi and Sonoda [39]	3.349	3.875	3.875	2.751	0.293	−0.293
	0.05	Present (21 × 21 points)	3.381	3.865	3.865	2.745	0.292	−0.292
		Kobayashi and Sonoda [39]	3.381	3.865	3.865	2.746	0.292	−0.292
	0.1	Present (21 × 21 points)	3.483	3.834	3.834	2.728	0.291	−0.291
		Kobayashi and Sonoda [39]	3.483	3.834	3.834	2.728	0.291	−0.291
	0.2	Present (21 × 21 points)	3.873	3.716	3.716	2.660	0.285	−0.285
		Kobayashi and Sonoda [39]	3.873	3.716	3.716	2.660	0.284	−0.284
5	0.01	Present (21 × 21 points)	1.505	1.545	1.552	1.458	0.174	−0.181
		Kobayashi and Sonoda [39]	1.506	1.540	1.540	1.462	0.176	−0.176
	0.05	Present (21 × 21 points)	1.509	1.526	1.526	1.452	0.176	−0.176
		Kobayashi and Sonoda [39]	1.509	1.526	1.526	1.452	0.175	−0.175
	0.1	Present (21 × 21 points)	1.519	1.482	1.482	1.421	0.173	−0.173
		Kobayashi and Sonoda [39]	1.519	1.482	1.482	1.421	0.172	−0.172
	0.2	Present (21 × 21 points)	1.551	1.328	1.328	1.311	0.162	−0.162
		Kobayashi and Sonoda [39]	1.551	1.328	1.328	1.311	0.162	−0.162

$$
\begin{aligned}
&+ kA_{45}\left(\sum_{j=1}^{N}\alpha_j^{\Psi_x}\phi_j + \sum_{j=1}^{N}\alpha_j^{W}\frac{\partial\phi_j}{\partial x}\right)\Bigg]\\
&-k_f\sum_{j=1}^{N}\alpha_j^{W}\phi_j + G_f\left(\sum_{j=1}^{N}\alpha_j^{W}\frac{\partial^2\phi_j}{\partial x^2} + \sum_{j=1}^{N}\alpha_j^{W}\frac{\partial^2\phi_j}{\partial y^2}\right)\\
&= -I_0\omega^2\sum_{j=1}^{N}\alpha_j^{W}\phi_j
\end{aligned}
\tag{49}
$$

where N represents the total number of points of the discretization. Vectors $\alpha_j^W, \alpha^{\Psi_x}, \alpha^{\Psi_y}$ correspond to the vector of unknowns related to translations W, and rotations Ψ_x, Ψ_y, respectively.

Boundary conditions can be discretized as follows. For a simply supported plate, along the perimeter we enforce the SS2 conditions as

$$
w = 0 \rightarrow \sum_{j=1}^{N}\alpha_j^{W}\phi_j = 0 \tag{50}
$$

$$
\begin{aligned}
M_n = 0 \rightarrow\ & n_x^2\left(D_{11}\sum_{j=1}^{N}\alpha_j^{\Psi_x}\frac{\partial\phi_j}{\partial x} + D_{12}\sum_{j=1}^{N}\alpha_j^{\Psi_y}\frac{\partial\phi_j}{\partial x}\right.\\
&\left. + D_{16}\sum_{j=1}^{N}\left(\alpha_j^{\Psi_y}\frac{\partial\phi_j}{\partial x} + \alpha_j^{\Psi_x}\frac{\partial\phi_j}{\partial y}\right)\right)\\
&+2n_xn_y\left(D_{16}\sum_{j=1}^{N}\alpha_j^{\Psi_x}\frac{\partial\phi_j}{\partial x} + D_{26}\sum_{j=1}^{N}\alpha_j^{\Psi_y}\frac{\partial\phi_j}{\partial x}\right.\\
&\left. +D_{66}\sum_{j=1}^{N}\left(\alpha_j^{\Psi_y}\frac{\partial\phi_j}{\partial x} + \alpha_j^{\Psi_x}\frac{\partial\phi_j}{\partial y}\right)\right)\\
&+n_y^2\left(D_{12}\sum_{j=1}^{N}\alpha_j^{\Psi_x}\frac{\partial\phi_j}{\partial x} + D_{22}\sum_{j=1}^{N}\alpha_j^{\Psi_y}\frac{\partial\phi_j}{\partial x}\right.\\
&\left. +D_{26}\sum_{j=1}^{N}\left(\alpha_j^{\Psi_y}\frac{\partial\phi_j}{\partial x} + \alpha_j^{\Psi_x}\frac{\partial\phi_j}{\partial y}\right)\right) = 0
\end{aligned}
\tag{51}
$$

$$
\theta_s = 0 \rightarrow n_x\sum_{j=1}^{N}\alpha_j^{\Psi_y}\phi_j + n_y\sum_{j=1}^{N}\alpha_j^{\Psi_x}\phi_j = 0. \tag{52}
$$

The eigenproblem is then defined as a generalized eigenproblem (19) or standard eigenproblem (22) and solved by MATLAB in our case.

Table 8 Deflections, moments and shear forces of uniformly loaded square CC plates on Winkler foundations ($\nu = 0.3$)

K	h/a	Method	w $(\times 10^{-3}qa^4/D)$ $x=y=0$	M_{xx} $(\times 10^{-2}qa^2/D)$ $x=y=0$	M_{yy} $(\times 10^{-2}qa^2/D)$ $x=y=0$	M_{xy} $(\times 10^{-2}qa^2/D)$ $x=y=-1$	Q_x $(\times qa)$ $x=0;\ y=-1$	Q_y $(\times qa)$ $x=-1, y=0$
1	0.01	Present (21 × 21 points)	1.868	2.629	2.876	0.094	0.408	–0.190
		Kobayashi and Sonoda [39]	1.918	2.437	3.320	0.101	0.244	–0.515
	0.05	Present (21 × 21 points)	1.989	2.471	3.322	0.467	0.244	–0.509
		Kobayashi and Sonoda [39]	1.989	2.472	3.321	0.466	0.245	–0.509
	0.1	Present (21 × 21 points)	2.206	2.575	3.321	0.850	0.248	–0.500
		Kobayashi and Sonoda [39]	2.206	2.575	3.321	0.850	0.245	–0.500
	0.2	Present (21 × 21 points)	3.015	2.915	3.298	1.433	0.256	–0.474
		Kobayashi and Sonoda [39]	3.015	2.915	3.298	1.433	0.256	–0.474
3	0.01	Present (21 × 21 points)	1.701	2.371	2.578	0.089	0.384	–0.174
		Kobayashi and Sonoda [39]	1.744	2.184	2.989	0.095	0.229	–0.480
	0.05	Present (21 × 21 points)	1.803	2.206	2.978	0.438	0.229	–0.474
		Kobayashi and Sonoda [39]	1.802	2.207	2.978	0.437	0.230	–0.474
	0.1	Present (21 × 21 points)	1.976	2.272	2.941	0.787	0.231	–0.462
		Kobayashi and Sonoda [39]	1.976	2.272	2.941	0.787	0.231	–0.462
	0.2	Present (21 × 21 points)	2.590	2.463	2.790	1.277	0.232	–0.425
		Kobayashi and Sonoda [39]	2.590	2.463	2.790	1.278	0.231	–0.425
5	0.01	Present (21 × 21 points)	1.047	1.369	1.423	0.067	0.291	–0.112
		Kobayashi and Sonoda [39]	1.069	1.212	1.709	0.073	0.172	–0.347
	0.05	Present (21 × 21 points)	1.088	1.204	1.673	0.326	0.170	–0.340
		Kobayashi and Sonoda [39]	1.088	1.204	1.673	0.326	0.171	–0.340
	0.1	Present (21 × 21 points)	1.141	1.181	1.569	0.556	0.167	–0.322
		Kobayashi and Sonoda [39]	1.141	1.181	1.569	0.556	0.167	–0.322
	0.2	Present (21 × 21 points)	1.289	1.098	1.252	0.788	0.154	–0.269
		Kobayashi and Sonoda [39]	1.289	1.098	1.252	0.788	0.154	–0.269

Table 9 Convergence of frequency parameters $\Delta_{1,1}$ for the flexural modes of thin and moderately thick square plates on Winkler foundation ($K_2 = 0$)

Boundary condition	t/b	K_1	13 × 13 points	17 × 17 points	21 × 21 points
SSSS ($\nu = 0.3$)	0.01	10^2	2.2444	2.2416	2.2414
		5×10^2	3.0238	3.0217	3.0215
	0.1	2×10^2	2.3990	2.3989	2.3989
		10^3	3.7008	3.7213	3.7213
CCCC ($\nu = 0.15$)	0.015	1390.2	5.3073	5.2440	5.2442
		2780.4	6.5141	6.4626	6.4627

5 Numerical examples

In all following examples a Chebyshev grid was used (in MATLAB : $x = cos(pi * (0 : N)/N)'$; $y = x$). The Wendland function used was

$$\phi(r) = (1 - cr)_+^8 \left(32(cr)^3 + 25(cr)^2 + 8cr + 1\right). \quad (53)$$

where the shape parameter is taken as 0.1.

5.1 Static results

Numerical results are presented for the uniformly loaded square plate ($a/b = 1$) for the various values of thickness-to-span ratio h/a and dimensionless foundation modulus $K = \left(k_f a^4/D\right)^{1/4}$. Here, $D = \frac{Eh^3}{12(1-\nu^2)}$ is the flexural rigidity. The Poisson's ratio of 0.3 is taken for all cases. In Tables 1, 2, 3 we present a convergence study for fully-clamped (CCCC) plates, using various thickness-to-side ratios, for $K = 1, 3,$ and $K = 5$. In Tables 4, 5, 6, we perform a similar convergence study for simply-supported (SSSS) plates. For both clamped and simply-supported plates the convergence is excellent. For thinner plates ($h/a = 0.01$) we need more

Table 10 Comparison of frequency parameters Δ for the flexural modes of thin and moderately thick square plates on Winkler foundation ($K_2 = 0$)

Boundary condition	t/b	K_1	Methods	$\Delta_{1,1}$	$\Delta_{1,2}$,$\Delta_{2,1}$	$\Delta_{2,2}$
SSSS ($\nu = 0.3$)	0.01	10^2	Zhou et al. [13]	2.2413	5.0973	8.0527
			Classical [3]	2.2420	5.1016	8.0639
			Mindlin [5]	2.2413	5.0971	8.0523
			Present (21×21 points)	2.2414	5.0967	8.0542
		5×10^2	Zhou et al. [13]	3.0214	5.4850	8.3035
			Classical [3]	3.0221	5.4894	8.3146
			Mindlin [5]	3.0215	5.4850	8.3032
			Present (21×21 points)	3.0216	5.4846	8.3051
	0.1	2×10^2	Zhou et al. [13]	2.3951	4.8262	7.2338
			Mindlin [5]	2.3989	4.8194	7.2093
			Present (21×21 points)	2.3989	4.8194	7.2093
		10^3	Zhou et al. [13]	3.7008	5.5661	7.7335
			Mindlin [5]	3.7212	5.5844	7.7353
			Present (21×21 points)	3.7213	5.5844	7.7353
CCCC ($\nu = 0.15$)	0.015	1390.2	Zhou et al. [13]	5.2446	8.3156	11.541
			Classical [3]	5.2510	8.3427	11.602
			Finite element [6]	5.2588	8.4322	11.674
			Present (21×21 points)	5.2438	8.3129	11.546
		2780.4	Zhou et al. [13]	6.4629	9.1324	12.142
			Classical [3]	6.4686	9.1582	12.202
			Finite element [6]	6.4601	9.2482	12.263
			Present (21×21 points)	6.4625	9.1302	12.147

Table 11 Comparison of frequency parameters Δ for the flexural modes of thin and moderately thick square plates on Pasternak foundation

Boundary condition	t/b	K_1	K_2	Methods	$\Delta_{1,1}$	$\Delta_{1,2}$,$\Delta_{2,1}$	$\Delta_{2,2}$
SSSS ($\nu = 0.3$)	0.01	10^2	10	Zhou et al. [13]	2.6551	5.5717	8.5406
				Mindlin [5]	2.6551	5.5718	8.5405
				Present (21×21 points)	2.6559	5.5718	8.5384
		5×10^2	10	Zhou et al. [13]	3.3398	5.9285	8.7775
				Mindlin [5]	3.3400	5.9287	8.7775
				Present (21×21 points)	3.3406	5.9285	8.7754
	0.1	2×10^2	10	Zhou et al. [13]	2.7756	5.2954	7.7279
				Mindlin [5]	2.7842	5.3043	7.7287
				Present (21×21 points)	2.7902	5.3452	7.8255
		10^3	10	Zhou et al. [13]	3.9566	5.9757	8.1954
				Mindlin [5]	3.9805	6.0078	8.2214
				Present (21×21 points)	3.9844	6.0430	8.3112
CCCC ($\nu = 0.15$)	0.015	1390.2	166.83	Zhou et al. [13]	8.1675	12.823	16.833
				Finite element [6]	8.1375	12.898	16.932
				Present (21×21 points)	8.1669	12.821	16.842

points than for thicker plates, to obtain an acceptable convergence of the transverse displacements.

The present method is compared with a Levy-type method by Kobayashi and Sonoda [39], Tables 7 and 8. Due to the Levy approach, edges $y = constant$ are simply-supported. The boundary conditions denoted by SS represent simply-supported bords along the perimeter, while CC indicates that the edges $y = constant$ are simply-supported and the opposite edges are clamped. From the convergence results in Tables 1, 2, 3, 4, 5, 6, it seems quite reasonable to use a 21×21 grid for all SSSS and CCCC cases. The results here presented show an excellent correlation with results by Kobayashi and Sonoda [39]. In most cases, results are identical, being the larger differences obtained for CCCC plates, and $h/a = 0.01$.

5.2 Free vibration results

Numerical results are presented for square plates ($a/b = 1$). The non-dimensional parameters are given as

$$\Delta = \frac{\omega b^2}{\pi^2}\sqrt{\rho t/D}, \quad K_1 = \frac{k_f a^4}{D}, \quad K_2 = \frac{G_f a^2}{D} \tag{54}$$

In Table 9 we present a convergence study of the frequency parameters $\Delta_{1,1}$ for the flexural modes of thin and moderately thick square plates on Winkler foundation ($K_2 = 0$). A 21×21 points grid was chosen to compare the present method with 3D results by Zhou et al. [13] who used a Ritz method to solve the three-dimensional problem of plates on Winkler foundations, Table 10. Natural frequencies are in excellent agreement with the Mindlin [5] results for thicker plates, and in good agreement with the results by Zhou et al. [13] and the classical results of Leissa [3] for thinner plates.

In Table 11 we present the frequency parameters Δ for the flexural modes of thin and moderately thick square plates on Pasternak foundation. We present results for SSSS and CCCC boundary conditions, and several values of K_1, K_2. We compare our results with those of Zhou et al. [13], using a 3D Ritz approach, and those of Xiang et al. [5] , who used a Mindlin approach. Our results are in excellent agreement with those of [5] and [13] in both SSSS and CCCC boundary conditions, and in both thin and thick plates.

In Figs. 1 and 2, we illustrate the eigenmodes for a CCCC plate, with $t/b = 0.015$, $K_1 = 2780.4$, using a 21×21 grid. The modes are quite stable.

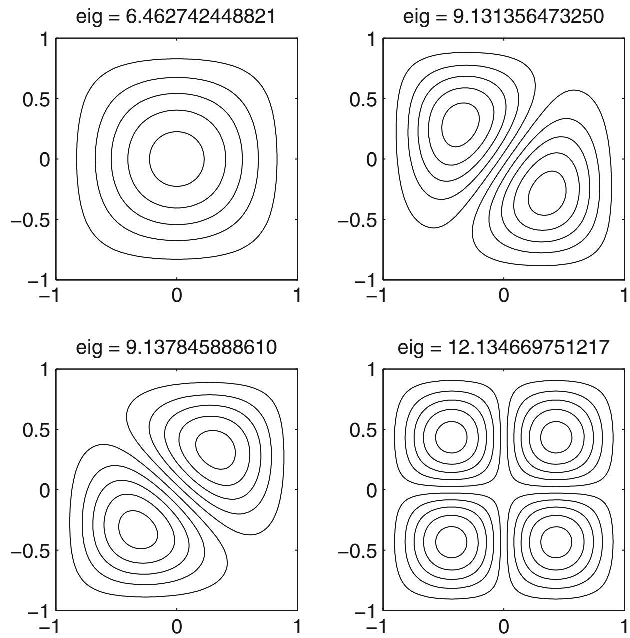

Fig. 1 First four vibrational modes: CCCC, $t/b = 0.015$, $K_1 = 2780.4$, grid 21×21

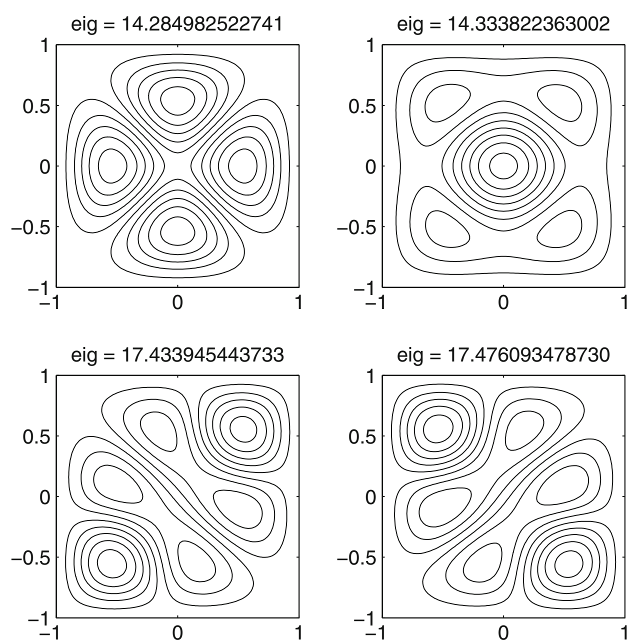

Fig. 2 Fifth to eighth vibrational modes: CCCC, $t/b = 0.015$, $K_1 = 2780.4$, grid 21×21

6 Conclusions

In this paper we used, for the first time, the RBF collocation method to analyse static deformations and free vibrations of plates on Pasternak foundations. The first-order shear deformation theory set of equations of motion define a static problem and an eigenproblem which can be solved by various algorithms.

The present results were compared with existing analytical solutions, and finite element schemes and are in very good agreement.

The present method is a simple yet powerful alternative to other finite element or meshless methods in the static deformation and free vibration analysis of plates on Pasternak foundations.

Acknowledgments The support of Ministério da Ciência Tecnologia e do Ensino Superior and Fundo Social Europeu (MCTES and FSE) under programs POPH-QREN are gratefully acknowledged.

References

1. Pasternak PL (1954) On a new method of analysis of an elastic foundation by means of two foundation constants. Gosudarstvennoe Izdatelstvo Literaturi po Stroitelstvu i Arkhitekture, Moscow, USSR, pp 1–56 (in Russian)
2. Winkler E (1867) Die Lehre von der Elasticitaet und Festigkeit. Prag, Dominicus
3. Leissa AW (1973) The free vibration of plates. J Sound Vib 31:257–293
4. Lam KY, Wang CM, He XQ (2000) Canonical exact solutions for levy-plates on two-parameter foundation using green's functions. Eng Struct 22:364–378
5. Xiang Y, Wang CM, Kitipornchai S (1994) Exact vibration solution for initially stressed Mindlin plates on pasternak foundation. Int J Mech Sci 36:311–316
6. Omurtag MH, Ozutok A, Akoz AY (1997) Free vibration analysis of kirchhoff plates resting on elastic foundation by mixed finite element formulation based on gateaux differential. Int J Numer Methods Eng 40:295–317
7. Matsunaga H (2000) Vibration and stability of thick plates on elastic foundations. J Eng Mech ASCE 126:27–34
8. Shen HS, Yang J, Zhang L (2001) Free and forced vibration of Reissner–Mindlin plates with free edges resting on elastic foundations. J Sound Vib 244:299–320
9. Ayvaz Y, Daloglu A, Dogangun A (1998) Application of a modified Vlasov model to earthquake analysis of plates resting on elastic foundations. J Sound Vib 212:499–509
10. Liew KM, Teo TM (2002) Differential cubature method for analysis of shear deformable rectangular plates on pasternak foundations. Int J Mech Sci 44:1179–1194
11. Liew KM, Han JB, Xiao ZM, Du H (1996) Differential quadrature method for Mindlin plates on winkler foundations. Int J Mech Sci 38:405–421
12. Han JB, Liew KM (1997) Numerical differential quadrature method for Reissner–Mindlin plates on two-parameter foundations. Int J Mech Sci 39:977–989
13. Zhou D, Cheung YK, Lo SH, Au FTK (2004) Three-dimensional vibration analysis of rectangular thick plates on pasternak foundation. Int J Numer Methods Eng 59:1313–1334
14. Civalek O, Acar MH (2007) Discrete singular convolution method for the analysis of Mindlin plates on elastic foundations. Int J Pres Vessel Pip 84:527–535
15. Chucheepsakul S, Chinnaboom B (2002) An alternative domain-boundary element technique for analyzing plates on two-parameter elastic foundations. Eng Anal Bound Elem 26:547–555
16. Kansa EJ (1990) Multiquadrics—a scattered data approximation scheme with applications to computational fluid dynamics. i: Surface approximations and partial derivative estimates. Comput Math Appl 19(8/9):127–145
17. Hon YC, Lu MW, Xue WM, Zhu YM (1997) Multiquadric method for the numerical solution of byphasic mixture model. Appl Math Comput 88:153–175
18. Hon YC, Cheung KF, Mao XZ, Kansa EJ (1999) A multiquadric solution for the shallow water equation. J Hydr Eng ASCE 125(5):524–533
19. Wang JG, Liu GR, Lin P (2002) Numerical analysis of biot's consolidation process by radial point interpolation method. Int J Solids Struct 39(6):1557–1573
20. Liu GR, Gu YT (2001) A local radial point interpolation method (LRPIM) for free vibration analyses of 2-d solids. J Sound Vib 246(1):29–46
21. Liu GR, Wang JG (2002) A point interpolation meshless method based on radial basis functions. Int J Numer Methods Eng 54:1623–1648
22. Wang JG, Liu GR (2002) On the optimal shape parameters of radial basis functions used for 2-d meshless methods. Comput Meth Appl Mech Eng 191:2611–2630
23. Chen XL, Liu GR, Lim SP (2003) An element free Galerkin method for the free vibration analysis of composite laminates of complicated shape. Compos Struct 59:279–289
24. Dai KY, Liu GR, Lim SP, Chen XL (2004) An element free Galerkin method for static and free vibration analysis of shear-deformable laminated composite plates. J Sound Vib 269:633–652
25. Liu GR, Chen XL (2002) Buckling of symmetrically laminated composite plates using the element-free Galerkin method. Int J Struct Stabil Dyn 2:281–294
26. Liew KM, Chen XL, Reddy JN (2004) Mesh-free radial basis function method for buckling analysis of non-uniformity loaded arbitrarily shaped shear deformable plates. Comput Meth Appl Mech Eng 193:205–225
27. Huang YQ, Li QS (2004) Bending and buckling analysis of antisymmetric laminates using the moving least square differential quadrature method. Comput Meth Appl Mech Eng 193:3471–3492
28. Liu L, Liu GR, Tan VCB (2002) Element free method for static and free vibration analysis of spatial thin shell structures. Comput Meth Appl Mech Eng 191:5923–5942
29. Ferreira AJM (2003) A formulation of the multiquadric radial basis function method for the analysis of laminated composite plates. Compos Struct 59:385–392
30. Ferreira AJM (2003) Thick composite beam analysis using a global meshless approximation based on radial basis functions. Mech Adv Mater Struct 10:271–284
31. Ferreira AJM, Roque CMC, Martins PALS (2003) Analysis of composite plates using higher-order shear deformation theory and a finite point formulation based on the multiquadric radial basis function method. Compos Part B Eng 34:627–636
32. Madich WR, Nelson SA (1990) Multivariate interpolation and conditionally positive definite functions. ii. Math Comp 54(189):211–230
33. Yoon J (2001) Spectral approximation orders of radial basis function interpolation on the sobolev space. SIAM J Math Anal 33(4):946–958
34. Hardy RL (1971) Multiquadric equations of topography and other irregular surfaces. J Geophys Res 176:1905–1915
35. Buhmann MD (2000) Radial basis functions. Acta Numer 9:1–38
36. Platte RB, Driscoll TA (2004) Computing eigenmodes of elliptic operators using radial basis functions. Comput Math Appl 48:561–576
37. Reddy JN (1997) Mechanics of laminated composite plates: theory and analysis. CRC Press, Boca Raton
38. Liew KM, Huang YQ, Reddy JN (2003) Vibration analysis of symmetrically laminated plates based on fsdt using the moving least squares differential quadrature method. Comput Meth Appl Mech Eng 192:2203–2222
39. Kobayashi H, Sonoda K (1989) Rectangular Mindlin plates on elastic foundation. Int J Mech Sci 31(9):679–692